HHS Public Access

Author manuscript

Stem Cells. Author manuscript; available in PMC 2016 May 25.

Published in final edited form as:

Stem Cells. 2014 January ; 32(1): 59–69. doi:10.1002/stem.1519.

The Subventricular Zone Is Able to Respond to a Demyelinating Lesion After Localized Radiation

Vivian Capilla-Gonzalez[a], **Hugo Guerrero-Cazares**[a], **Janice M. Bonsu**[a], **Oscar Gonzalez-Perez**[b], **Pragathi Achanta**[a], **John Wong**[c], **Jose Manuel Garcia-Verdugo**[d], and **Alfredo Quiñones-Hinojosa**[a]

[a]Brain Tumor Stem Cell Laboratory, Department of Neurosurgery, Johns Hopkins School of Medicine, Baltimore, Maryland, USA

[b]Neuroscience Laboratory, Psychology School, University of Colima, Colima, Mexico

[c]Radiation Oncology and Molecular Radiation Sciences, Johns Hopkins School of Medicine, Baltimore, Maryland, USA

[d]Laboratory of Comparative Neurobiology, Instituto Cavanilles de Biodiversidad y Biologia Evolutiva, University of Valencia, CIBERNED, Paterna, Valencia, Spain

Abstract

Radiation is a common tool in the treatment of brain tumors that induces neurological deficits as a side effect. Some of these deficits appear to be related to the impact of radiation on the neurogenic niches, producing a drastic decrease in the proliferative capacity of these regions. In the adult mammalian brain, the subventricular zone (SVZ) of the lateral ventricles is the main neurogenic niche. Neural stem/precursor cells (NSCs) within the SVZ play an important role in brain repair following injuries. However, the irradiated NSCs' ability to respond to damage has not been previously elucidated. In this study, we evaluated the effects of localized radiation on the SVZ ability to respond to a lysolecithin-induced demyelination of the striatum. We demonstrated that the proliferation rate of the irradiated SVZ was increased after brain damage and that residual NSCs were reactivated. The irradiated SVZ had an expansion of doublecortin positive cells that appeared to migrate from the lateral ventricles toward the demyelinated striatum, where newly generated oligodendrocytes were found. In addition, in the absence of demyelinating damage, remaining cells in the irradiated SVZ appeared to repopulate the neurogenic niche a year post-radiation. These findings support the hypothesis that NSCs are radioresistant and can respond to a brain injury, recovering the neurogenic niche. A more complete understanding of the effects that

Correspondence: Alfredo Quiñones-Hinojosa, M.D., Department of Neurosurgery, Johns Hopkins University, 1550 Orleans Street, CRB-II, Room 247, Baltimore, Maryland 21201, USA. Telephone: +1-410-502-2869; Fax: +1-410-502-7559; ; Email: aquinon2@jhmi.edu

Author Contributions: V.C.G.: collection and/or assembly of data, conception and design, data analysis and interpretation, manuscript writing, and final approval of manuscript; H.G.C.: data analysis and interpretation, manuscript writing, and final approval of manuscript; J.M.B.: collection and/or assembly of data; O.G.P.: data analysis and interpretation; P.A.: collection and/or assembly of data and assisted with SARRP technology; J.W.: provided SARRP technology; J.M.G.V. and A.Q.H.: data analysis and interpretation, final approval of manuscript, and financial support.

Disclosure of Potential Conflicts of Interest: Dr. John Wong has a sponsored research agreement and consultation agreement with Xstrahl, who currently commercializes the SARRP. Despite that, the authors indicate no potential conflict of interest.

localized radiation has on the SVZ may lead to improvement of the current protocols used in the radiotherapy of cancer.

Keywords

Subventricular zone; Neural stem cells; Radiation; Lysolecithin; Oligodendrogenesis; Brain Damage; Demyelinating diseases

Introduction

Radiation therapy is one of the most widely used therapies for brain tumor patients [1, 2]. Side effects of brain tumor radiotherapy frequently include neurological deficits of clinical relevance, such as cognitive and psychological dysfunction [3–5]. These effects are largely due to the impossibility to circumvent the normal brain, specifically the neurogenic niches, during radiation [6–8]. In the adult mammalian brain, including humans, the subventricular zone (SVZ) constitutes the main neurogenic niche [9, 10]. This area serves as a source of neural stem/precursor cells (NSCs) with the ability to proliferate and differentiate into astrocytes, neurons, or oligodendrocytes [11–15]. In the SVZ, NSCs correspond to a subset of astrocytes called type B1 cells that retain an apical contact with the ventricle [16, 17]. NSCs proliferate and give rise to intermediate progenitors (type C cells), which in turn generate neuroblasts (type A cells) [18]. From the SVZ, neuroblasts migrate tangentially through the rostral migratory stream (RMS) to the olfactory bulb, where they differentiate into mature neurons [19, 20]. Additionally, a small subset of NSCs generates oligodendrocyte precursor cells, which migrate radially to periventricular areas such as the corpus callosum, septum, or striatum and differentiate into myelinating oligodendrocytes [14, 21, 22]. Besides supporting constitutive neurogenesis and oligodendrogenesis, the SVZ has the ability to respond to brain damage by activating repair mechanisms [23–28]. For instance, after a stroke and demyelinating damage, new cells are generated and mobilized from the SVZ to the site of the injury, where they differentiate into neurons and myelinating oligodendrocytes, respectively [14, 21, 24, 26, 29–33].

It is well-established that radiation depletes the cell populations in the SVZ and reduces its proliferative and neurogenic capacity [34–36]. Using a novel small animal radiation research platform (SARRP) that more accurately reproduces human radiotherapy [37–40], our group recently demonstrated that a subset of NSCs is maintained in the locally irradiated SVZ of adult mice [38]. However, the functionality of these NSCs and their ability to respond to subsequent brain damage has not yet been investigated. In this study, we assessed the capacity of the localized irradiated SVZ to respond to a demyelinating brain lesion induced by lysolecithin (Lys) injection. Our results indicate that the remaining NSCs within the SVZ can actively respond to the injury despite radiation. Following Lys injection, the neuroblasts expanded from the irradiated SVZ toward the lesion site, forming migratory chain-like structures. The injured hemisphere displayed an increase in the number of newly generated cells, which frequently express the early-stage oligodendrocyte marker Olig2. In addition, we found that, in the absence of a demyelinating damage, the remaining cells from the locally irradiated SVZ are able to repopulate the neurogenic niche a year after radiation.

Since a complete irradiation of the brain disrupts the environment by altering either the production of growth factors or the integrity of blood vessels [41–43], it is important to target the SVZ specifically, without affecting the neighboring brain parenchyma. To our knowledge, this is the first study that analyzes the capacity of the SVZ to respond to brain damage following localized radiation by specifically targeting the SVZ. The detailed understanding of the effects that radiation has on the neurogenic niches may lead to the development of new strategies to minimize radiotherapy-related effects in patients requiring brain radiation.

Materials and Methods

Animal Subjects

The animals used in this study were 2-month-old C57BL/6 male mice from the National Cancer Institute and the National Institute on Aging (Baltimore, MD). All the animals (n = 39) were housed under a 12-hour light/dark cycle with food and water available ad libitum (see Supporting Information Table S1 for experimental groups information). All experiments described were performed with the approval of the Johns Hopkins Animal Care and Use Committee under standard animal care and use protocols.

Localized Brain Irradiation

Radiation was delivered to the mice using the SARRP, a precision radiation device based on computed tomography (CT) images [36–39]. Radiation co-ordinates to target the SVZ were established by visualizing the ventricles via iodine-contrasted CT scan, as described previously by our group [37, 39]. Mice were anesthetized with an injection of 100 mg/kg ketamine + 10 mg/kg xylazine via intraperitoneal. Then, a single dose of 10 Gy was delivered using computed tomography-based tissue visualization. A radiation beam of 3 mm × 3 mm was used to target the right SVZ, while the left brain structures served as controls. We have previously demonstrated the specific targeting of the mouse SVZ by immunostaining against the phosphorylated histone H2AX (c-H2AX), a marker of DNA double-strand breaks [38, 39]. Radiation effects were first evaluated at 30 days after radiation delivery. For the model combining radiation and Lys injection, animals were euthanized 60 days after radiation. For the long-term survival model, animals were euthanized a year post-radiation.

Demyelinating Lesion

Demyelination of the striatum was induced by injecting Lys (Sigma-Aldrich, St. Louis, MO, http://www.sigmaaldrich.com), as described previously [32]. A volume of 0.5 μL of 1% Lys in 0.9% sodium chloride was injected into the right striatum (coordinates L 1.5, A 0.8, D 3.3 relative to bregma). A group of animals was injected with 0.9% saline to serve as control for the intracranial injection. Lys effects were first evaluated at different time points (0, 3, 15, and 30 days). For the model combining radiation and Lys injection, animals were euthanized 30 days after Lys treatment.

Administration of BrdU

To label the dividing cells after irradiation, we used the 5-bromo-2′-deoxyuridine (BrdU) (Sigma-Aldrich). Prior to Lys-treatment, animals received four intraperitoneal injections of BrdU (50 mg/kg b.wt.), separated by 2 hours, and were sacrificed 31 days after. This protocol allowed to label the subset of cells that were proliferating after radiation delivery, as well as a portion of the cells that were generated in response to local brain damage.

Brain Tissue Fixation

Animals were anesthetized by an intraperitoneal injection of 100 mg/kg ketamine + 10 mg/kg xylazine. Then, mice were subjected to an intracardiac perfusion using a peristaltic pump. As a fixative, we used 2% paraformaldehyde and 2.5% glutaraldehyde for electron microscopy or 4% paraformaldehyde for immunohistochemistry. Before brain dissection, heads were removed and postfixed in the same fixative overnight.

Transmission Electron Microscopy

After postfixation, brains were washed in 0.1 M phosphate buffer (PB) (pH 7.4), cut into 200 μm sections with a VT 1000M vibratome (Leica, Wetzlar, Germany, http://www.leica.com), and treated with 2% osmium tetraoxide in 0.1 M PB for 2 hours. Then, sections were rinsed, dehydrated through increasing ethanol solutions, and stained in 2% uranyl acetate at 70% ethanol. Following dehydration, slices were embedded in araldite (Durcupan, Fluka BioChemika, Ronkokoma, NY, http://www.sigmaaldrich.com). To study the cell organization, we cut serial 1.5 μm semithin sections with a diamond knife and stained them with 1% toluidine blue. To analyze ultra-structure features, 60–70 nm ultrathin sections were cut with a diamond knife, stained with lead citrate, and examined under a Spirit transmission electron microscope (FEI Tecnai, Hillsboro, OR, http://www.fei.com/products/tem/tecnai).

Immunohistochemistry

After postfixation, brains were washed in 0.1 M PB and cut into serial 10 μm thick coronal sections using a cryostat (Leica, CM 1900). One series (5–8 sections) from each animal was used in each immunostaining. Sections were incubated in blocking solution for 1 hour at room temperature, followed by overnight incubation at 4°C with primary antibodies (Table 1). Then, sections were washed and incubated with the appropriate secondary antibodies conjugated with fluorophores, examined under a Zeiss Axio Observed Z1microscope, and imaged with the AxioVision software version 4.8. (Oberkochen, Germany, http://www.zeiss.com). Confocal images were captured using a Zeiss LSM 710 confocal microscope.

Cell Quantification

The quantifications of Ki67, Mash1, and Olig 2+ cells along the ventricle wall were assayed in SVZ coronal sections and expressed as cells per mm. Measurement of BrdU incorporation was carried out in coronal sections by quantification of BrdU+ cells, considering the area comprised in the first 500 mm adjacent to the ventricle lumen. Results were expressed as cells per section. Quantification of BrdU/Olig2+ cells was expressed as the percentage of double positive cells of the total of BrdU+ cells found in the same area (100 × BrdU-Olig2+

cells/total BrdU+ cells). Quantification of Ki67/Sox2+ cells was expressed as the percentage of double positive cells of the total of Ki67+ cells found in the same area (100 × Ki67-Sox2+ cells/total Ki67+ cells). Quantification of the glial fibrillary acidic protein (GFAP) and doublecortin (DCX) was assayed in coronal sections by measuring the integrated density with ImageJ software (National Institute of Mental Health, Bethesda, MD, http://rsbweb.nih.gov/ij) [66].

Statistical Analysis

Data was expressed as mean ± SEM and analyzed using the SigmaPlot 11.0 software (Jandel Scientific, San Rafael, CA, http://www.sigmaplot.com/products/sigmaplot). Student's *t* test was performed to compare two experimental groups, while one-way ANOVA was performed to compare multiple groups. The differences were considered significant at a p value less than .05.

Results

NSCs within the Irradiated SVZ Are Able to Proliferate in Response to a Demyelinating Injury

To determine if localized radiation affects the ability of the SVZ to respond to injuries, we combined localized radiation and Lys injection in a single mouse model. The effectiveness of radiation and Lys-treatment were separately verified by immunostaining and electron microscopy. First, the SVZ showed a notable disruption of its proliferative capacity 30 days after localized radiation (Supporting Information Fig. S1) and a decrease of total SVZ cells (non-Irr SVZ: 236.1 ± 26.2 cells per mm, Irr SVZ: 97.9 ± 6 cells per mm, $p < .001$). While type C and A cells were depleted after radiation, type B cells were not affected in the SVZ, preserving astrocyte-like NSCs (type B1 cells) (Supporting Information Fig. S2). On the other hand, the striatum injected with Lys displayed myelin degeneration 3 days after treatment, and a disrupted expression of the myelin basic protein (MBP), an integral component of myelin, 15 days after Lys administration (Supporting Information Fig. S3). In accordance with previous studies [21, 32], the demyelinating lesion induced the activation of the SVZ over time (Supporting Information Fig. S4). The data indicate that our model is suitable to evaluate if the irradiated SVZ responds to a demyelinating damage.

Subsequently, localized radiation was delivered in the right hemisphere, followed by Lys-treatment (Fig. 1A, 1B). Cell proliferation was then assessed by immunostaining against Ki67. We found that the irradiated SVZ of mice injected with saline (Irr-saline) had a significant decrease of Ki67+ cells when compared to the non-irradiated (non-Irr) SVZ, consistent with our previous data (Supporting Information Fig. S1 and [38]). Interestingly, the injection of Lys in the irradiated hemisphere (Irr-Lys) induced an increase in the number of Ki67+ cells, compared to the non-Irr SVZ. However, the number of Ki67+ cells was lower than in the non-irradiated hemisphere that received Lys (Non-Irr 74.19 ± 12.25 cells per mm, Irr-Saline 41.77 ± 9.6 cells per mm, Irr-Lys 103.54 ± 9.5 cells per mm, Lys 143.95 ± 3.58 cells per mm, all comparisons with $p < .05$) (Fig. 1C). Ki67+ cells were observed between the SVZ and the adjacent striatum of the Irr-Lys hemisphere, similar to the Lys hemisphere, which was not observed in the groups without demyelination (Fig. 1D). Next,

the NSC population was examined by immunostaining against Nestin and Sox2. Cells expressing Nestin and Sox2 markers were observed in the SVZ of all experimental groups. However, frequent Nestin+ and Sox2+ cells were found in the adjacent striatum of the Irr-Lys hemisphere, similar to the Lys hemisphere (Fig. 1E; Supporting Information Fig. S5). In order to evaluate if NSCs were proliferative, we performed double immunostaining against Ki67/Nestin and Ki67/Sox2. Ki67+ cells were observed coexpressing Nestin and Sox2+ cells in the SVZ and the striatum of the Irr-Lys hemisphere (Fig. 1F and Supporting Information Fig. S5), as we observed in the Lys hemisphere (inset in Supporting Information Fig. S4E). However, the percentage of proliferative NSCs within the SVZ showed no significant differences between groups (Non-Irr 9.66 ± 2.29%, Irr-Saline 6.91±1.35%, Irr-Lys 7.96±3.12%, Lys 11.01 ± 1.78%, all comparisons with $p > .05$) (Supporting Information Fig. S5). Together, these findings suggest that SVZ cells are able to undergo mitosis in response to Lys-treatment, despite receiving localized radiation.

Neuroblasts Were Found in the Demyelinated Site Forming Migratory Chain-Like Structures

After observing that radiation did not prevent the activation of SVZ cells in response to demyelinating damage, we wondered whether their migratory patterns were affected. For this purpose, the neuroblasts population was examined by using the marker DCX. While radiation induced a depletion of DCX+ cells in the Irr-Saline SVZ as compared to the Non-Irr SVZ, the Irr-Lys SVZ had an increased expression of DCX. Remarkably, we observed the DCX stain in the demyelinated striatum in both the Irr-Lys and the Lys hemispheres (Fig. 2A–2D). When examining the DCX+ cells of the Irr-Lys hemisphere in detail (Fig. 2E), we found that the neuroblasts located in the SVZ appear to project their cellular processes toward the adjacent parenchyma (details 1a and 1b in Fig. 2). Ectopic DCX+ cells in the striatum of the Irr-Lys hemisphere had an elongated morphology and were found as individual cells or forming migratory chain-like structures (details 2 and 3 in Fig. 2). Those chains of neuroblasts were parallel to the ventricle wall and seemed to originate from the dorsal horn and the ventral part of the SVZ. In addition, the ectopic DCX+ cells located in the striatum coexpressed Nestin in both Irr-Lys and Lys groups (Fig. 2F, 2G). Together, these findings suggest that neuroblasts could migrate from the irradiated SVZ toward the site of injury.

We then examined the RMS of the Irr-Lys hemisphere and found an increase in the expression of DCX as compared to the Non-Irr hemisphere. Contrarily, the saline injection in the irradiated hemisphere did not produce an increase in the DCX expression when compared to Non-Irr hemisphere (Supporting Information Fig. S6A). These findings provide additional evidence that the Lys-induced lesion increased the number of migrating neuroblasts in the Irr-Lys hemisphere, which may follow their typical migratory route through the RMS toward the olfactory bulb.

The Production of New Cells Was Increased in the SVZ and Adjacent Striatum of the Irr-Lys Hemisphere

The adult brain has the ability to generate new oligodendrocytes when a demyelinating lesion occurs [21, 32]. To investigate whether the irradiated brain preserves this capacity,

irradiated animals were injected with four doses of BrdU the day before Lys-treatment (Fig. 3A), and double immunostaining against BrdU and Olig2 was carried out. The SVZ and adjacent striatum of the Irr-Lys hemisphere had a significant increase in the number of BrdU + cells, compared to the non-irradiated and the Irr-Saline hemisphere (Non-Irr 4.54 ± 0.76 cells, Irr-Saline 4 ± 0.76 cells, Irr-Lys 17.66 ± 4.26 cells, $p < .05$ comparing Irr-Lys vs. all other treatments) (Fig. 3B), but we did not find differences in the number of Olig2+ cells between groups (Non-Irr 219.58 ± 25.2 cells, Irr-Saline 201.16 ± 6.5 cells, Irr-Lys 191.33 ± 39.28 cells, all comparisons with $p > .05$) (Fig. 3C). Next, we analyzed the number of BrdU-Olig2+ cells and observed a significant increase in the SVZ and adjacent striatum of the Irr-Lys hemisphere compared to the non-irradiated hemisphere, and an increasing trend compared to the Irr-Saline hemisphere (Non-Irr 1.63±0.39 cells, Irr-Saline 1.167 ± 0.726 cells, Irr-Lys 3.167 ± 1.878 cells, $p < .05$ comparing Irr-Lys vs. Non-Irr) (Fig. 3D–3H). These findings indicate that the Irr-Lys hemisphere preserves the ability to produce immature oligodendrocytes after radiation.

Typically, a demyelinating lesion is characterized by a degradation of the myelin sheaths, showing a discontinuous and fragmented expression of MBP (Fig. 3I). When we examined the MBP expression in the striatum of the Irr-Lys hemisphere, we observed that the MBP staining appears continuous, similar to the Irr-Saline hemisphere (Fig. 3J, 3K). This result suggests that myelin repair may occur after demyelinating damage in the irradiated hemisphere.

The SVZ Is Repopulated a Year After Localized Radiation in the Absence of Damage

The fact that the irradiated SVZ was able to respond to the demyelinating lesion raised the question of whether our localized radiation model presents permanent effects in the SVZ cells. Previously, we demonstrated that radiation depletes all population of SVZ cells 30 days after delivery (Supporting Information Fig. S2 and [38]). Now, we evaluated the irradiated SVZ, 1 year after irradiation (Fig. 4A, 4B). The main SVZ cell subtypes were examined by using GFAP, DCX, Mash1, and Olig2 markers as described previously [44]. The expression of those markers showed no differences between the non-irradiated and irradiated SVZ (Fig. 4C–4J). Subsequently, SVZ proliferative capacity was evaluated using immunostaining against Ki67. Despite of the repopulation of the SVZ, we found a 38% reduction in the number of proliferative cells presented in the irradiated SVZ a year post-radiation, as compared to the non-irradiated SVZ (Non-Irr 41.20 ± 1.99 cells per mm, Irr 25.63 ± 3.985 cells per mm, $p = .025$) (Fig. 5A–5C). Cells coexpressing Ki67 and the NSC marker Nestin were observed in the irradiated SVZ, suggesting that proliferative NSCs are preserved a year post-radiation (Fig. 5D). Together, these results suggest that the proliferative cells that remain in the irradiated SVZ may partially recover the effects of localized radiation over time by repopulating the SVZ.

When we examined the RMS of mice a year post-radiation, we also found that the DCX expression was regained, showing no differences between the irradiated and non-irradiated hemisphere (Non-Irr 94.99 ± 1.48 integrated density, Irr 93.56 ± 1.23 integrated density, $p = .501$) (Supporting Information Fig. S6). This result suggests that the time span of one year allows the SVZ niche to recover its capacity of neuroblasts production.

Discussion

Although numerous reports demonstrate that radiation impacts the NSC population [7, 8, 38, 45, 46], the functionality of the NSCs that remain after radiation had not previously been investigated. In this study, we used a novel localized radiation model combined with a subsequent demyelinating lesion to investigate how radiation affects the endogenous regenerative capacity of the SVZ in the adult brain. We demonstrated that, despite receiving localized radiation, NSCs within the SVZ have the remarkable ability to respond to a demyelinating lesion. The main findings of this study pertain to the radioresistance property of the NSCs.

Locally Irradiated SVZ Is Able to Respond to a Lys-Induced Demyelinating Lesion

The NSCs residing in the SVZ have the ability to produce new cells capable of migration and regeneration following brain damage [23, 24, 47]. In the human brain, the physiological role of the SVZ neurogenesis is not fully understood, since migration of the SVZ-derived neuroblasts toward the olfactory bulb remains controversial [48–51]. However, the SVZ neurogenic niche maintains its capacity to respond to a brain damage in humans [26, 30, 52]. For instance, ischemia induced an increase in the number of proliferating and migrating cells in the ipsilateral SVZ of patients [30, 52]. Unfortunately, SVZ radiation could compromise this intrinsic regenerative ability, since a partial depletion of precursor cells following radiation delivery has been observed in animal models [7, 8, 35, 38]. We previously demonstrated a decrease in the proliferative and neurogenic capacity of the mouse SVZ after localized radiation using our novel SARRP technology [38]. We now report that the irradiated SVZ is able to respond to a brain injury with an increase in the number of proliferating cells and neuroblasts. These proliferative and migrating responses of the SVZ progenitors may be due to the local production of diffusible growth factors or inflammatory cytokines, which strongly regulate the function of NSCs [53–57].

In the Irr-Lys hemispheres, some proliferative cells coexpressed markers of NSCs, such as Nestin or Sox2. However, the number of proliferative NSCs showed no differences between groups, likely due to the fact that other progenitor cells were contributing to the pool of SVZ proliferative cells. This could explain the increase in the neuroblasts population that was found in the irradiated SVZ after Lys treatment. Together, these results demonstrate that, in our model, the localized radiation does not prevent the SVZ response to brain damage.

SVZ-Derived Cells Could Contribute to Repair the Demyelinating Lesion After Localized Radiation

The recruitment of new cells into the lesion area has been previously reported in multiple sclerosis patients [26] as well as in demyelinating animal models [21, 34, 58]. In our study, ectopic neuroblasts were observed in the lesion site as individual cells or forming migratory chain-like structures, similar to the neuroblast chains described in the RMS [20]. By specifically targeting SVZ primary precursors with retroviruses that express the reporter gene green fluorescent protein, it was demonstrated that the SVZ-derived cells migrate toward the corpus callosum when an injury is induced by local administration of Lys [32, 58]. Consistent with these studies, we observed massive neuroblasts forming chains in the

hemispheres treated with Lys. These neuroblasts emerged from the ventral SVZ and went into the striatum. Based on our finding and the previous studies, we consider that the ectopic neuroblasts that we found in the striatum of the Irr-Lys hemisphere could also be migrating from the SVZ. The location and morphology of these neuroblasts also support this idea. Our results suggest that the remaining NSCs in the locally irradiated SVZ can not only divide but also produce neuroblasts that appear to migrate into the lesion site.

The SVZ-derived cells recruited at the lesion site have been suggested to participate in remyelination after stimulation with the epidermal growth factor, recovering from the myelin damage at 14 and 28 days postlesion [32]. Here, we found that the myelin in the striatum of the Irr-Lys hemisphere appears to regenerate 30 days after Lys-treatment, in accordance with the MBP expression pattern. This result is supported by the finding of an increased number of newly generated cells in the Irr-Lys hemisphere, some of which were identified as immature oligodendrocytes. Following Lys-induced demyelination in the corpus callosum, SVZ-derived DCX positive cells were found to redirect from neuronal to glial fates, generating new oligodendrocytes in the injury site [58]. Based on this study, we suggest that the ectopic DCX positive cells found in the Irr-Lys hemisphere could be generating new cells of the oligodendroglial lineage that may participate in the brain repair. However, this study has a limitation to conclude myelin regeneration. First, by analyzing the MBP staining, we are not examining the myelin sheaths. Second, the MBP staining could be affected by the preservation of the tissue, and a poor or inadequate fixation could lead to an incorrect interpretation of the staining patterns. Further works are necessary to determine if the irradiated SVZ is able to regenerate a demyelinated injury.

NSCs Within the SVZ Have Radioresistant Properties

The limited impact of radiation on the NSC population could be associated to the radioresistant property of these cells. Stem cells from different organs have been proposed to be radiation resistant due to their highly effective mechanisms capable of repairing DNA damage [59–62]. Moreover, the radioresistance could also be attributed to the low dividing activity of the stem cells. In the adult SVZ, the most common dividing cells are the intermediate progenitors (type C cells), followed by neuroblasts (type A cells), while the type B cells (astrocytes-like NSCs) are the least dividing cell population. Similarly, the cell cycle length is shorter in the type B cells, compared to type C and A cells [63]. These findings imply that the DNA of the type B cells is less exposed to damaging factors than other proliferative SVZ cells. Consistent with this, the exposure to *N*-ethyl-*N*-nitrosourea, a mutagen that affects dividing cells, induced a reduction of intermediate progenitors and neuroblasts, while the type B cells were unaltered [64–66]. Highly proliferative populations were also depleted from the SVZ following a treatment with the antimitotic drug cytosine-*b*-D-arabinofuranoside, while some astrocytes were preserved [18]. In both cases, the SVZ was found to regenerate after a recovery period [18, 65]. Our study shows that, in our model, the effects of localized radiation on the proliferation and neurogenic properties of the SVZ are not permanent. The irradiated SVZ preserved proliferative NSCs that are not only able to respond to a brain injury but also repopulate the neurogenic niche a year after radiation. These findings provide new evidence for the radioresistance of NSCs in our model, where radiation is locally delivered to the SVZ. Although we cannot rule out the possibility that

NSCs from non-irradiated levels can be participating in the regenerative effects described in this study, the presence of proliferative NSCs in the irradiated SVZ supports our hypothesis.

Conclusion

Our results demonstrate that the locally irradiated SVZ preserves NSCs capable to respond to a demyelinating lesion in the striatum by increasing the number of proliferative cells and neuroblasts. Newly generated cells were found in the irradiated SVZ and adjacent striatum that differentiate into the oligodendrocyte lineage, which is crucial to repair demyelinating lesions. Furthermore, the remaining cells in the irradiated SVZ appeared to repopulate the neurogenic niche a year post localized radiation in the absence of damage. Our results support the hypothesis that NSCs are resistant to SVZ radiation. Increasing the understanding of how local radiation affects the SVZ could improve current radiotherapy protocols used in the treatment of patients.

Supplementary Material

Refer to Web version on PubMed Central for supplementary material.

Acknowledgments

We thank Gerald Son and Hongjun Song for their technical help with the confocal microscope, Eric Ford for his assistance with SARRP technology, and Sean Dangelmajer for his proof and critical reading of the manuscript. This research was supported by the National Institutes of Health-RO1 NS070024 and the Maryland Stem Cell Research Fund (A.Q.H. and H.G.C.), the Robert Wood Johnson Foundation (A.Q.H.), the Howard Hughes Medical Institute (A.Q.H.), the Prometeo grant GVPROMETEO-2009/011 (J.M.G.V.), the Red de TerapiaCelularTerCel—RETICS—from Instituto de Salud Carlos III (J.M.G.V.), the MINECO-SAF2012-33683 (J.M.G.V.), and the Consejo Nacional de Ciencia y Tecnologia CONACyT-2008-101476 (O.G.P.).

References

1. Stupp R, Hegi ME, Mason WP, et al. Effects of radiotherapy with concomitant and adjuvant temozolomide versus radiotherapy alone on survival in glioblastoma in a randomised phase III study: 5-year analysis of the EORTC-NCIC trial. Lancet Oncol. 2009; 10:459–466. [PubMed: 19269895]
2. Stupp R, Mason WP, van den Bent MJ, et al. Radiotherapy plus concomitant and adjuvant temozolomide for glioblastoma. N Engl J Med. 2005; 352:987–996. [PubMed: 15758009]
3. Calabrese P, Schlegel U. Neurotoxicity of treatment. Recent Results Cancer Res. 2009; 171:165–174. [PubMed: 19322544]
4. Marazziti D, Baroni S, Catena-Dell'osso M, et al. Cognitive, psychological and psychiatric effects of ionizing radiation exposure. Curr Med Chem. 2012; 19:1864–1869. [PubMed: 22376039]
5. Dietrich J, Monje M, Wefel J, et al. Clinical patterns and biological correlates of cognitive dysfunction associated with cancer therapy. Oncologist. 2008; 13:1285–1295. [PubMed: 19019972]
6. Achanta P, Fuss M, Martinez JL Jr. Ionizing radiation impairs the formation of trace fear memories and reduces hippocampal neurogenesis. Behav Neurosci. 2009; 123:1036–1045. [PubMed: 19824769]
7. Tada E, Parent JM, Lowenstein DH, et al. X-irradiation causes a prolonged reduction in cell proliferation in the dentate gyrus of adult rats. Neuroscience. 2000; 99:33–41. [PubMed: 10924950]
8. Monje ML, Mizumatsu S, Fike JR, et al. Irradiation induces neural precursor-cell dysfunction. Nat Med. 2002; 8:955–962. [PubMed: 12161748]

9. Doetsch F, Garcia-Verdugo JM, Alvarez-Buylla A. Cellular composition and three-dimensional organization of the subventricular germinal zone in the adult mammalian brain. J Neurosci. 1997; 17:5046–5061. [PubMed: 9185542]
10. Quinones-Hinojosa A, Sanai N, Soriano-Navarro M, et al. Cellular composition and cytoarchitecture of the adult human subventricular zone: A niche of neural stem cells. J Comp Neurol. 2006; 494:415–434. [PubMed: 16320258]
11. Abrous DN, Koehl M, Le Moal M. Adult neurogenesis: From precursors to network and physiology. Physiol Rev. 2005; 85:523–569. [PubMed: 15788705]
12. Alvarez-Buylla A, Garcia-Verdugo JM. Neurogenesis in adult subventricular zone. J Neurosci. 2002; 22:629–634. [PubMed: 11826091]
13. Ming GL, Song H. Adult neurogenesis in the mammalian central nervous system. Annu Rev Neurosci. 2005; 28:223–250. [PubMed: 16022595]
14. Menn B, Garcia-Verdugo JM, Yaschine C, et al. Origin of oligodendrocytes in the subventricular zone of the adult brain. J Neurosci. 2006; 26:7907–7918. [PubMed: 16870736]
15. Sanai N, Tramontin AD, Quinones-Hinojosa A, et al. Unique astrocyte ribbon in adult human brain contains neural stem cells but lacks chain migration. Nature. 2004; 427:740–744. [PubMed: 14973487]
16. Doetsch F, Caille I, Lim DA, et al. Subventricular zone astrocytes are neural stem cells in the adult mammalian brain. Cell. 1999; 97:703–716. [PubMed: 10380923]
17. Mirzadeh Z, Merkle FT, Soriano-Navarro M, et al. Neural stem cells confer unique pinwheel architecture to the ventricular surface in neurogenic regions of the adult brain. Cell Stem cell. 2008; 3:265–278. [PubMed: 18786414]
18. Doetsch F, Garcia-Verdugo JM, Alvarez-Buylla A. Regeneration of a germinal layer in the adult mammalian brain. Proc Natl Acad Sci USA. 1999; 96:11619–11624. [PubMed: 10500226]
19. Carleton A, Petreanu LT, Lansford R, et al. Becoming a new neuron in the adult olfactory bulb. Nat Neurosci. 2003; 6:507–518. [PubMed: 12704391]
20. Lois C, Garcia-Verdugo JM, Alvarez-Buylla A. Chain migration of neuronal precursors. Science. 1996; 271:978–981. [PubMed: 8584933]
21. Nait-Oumesmar B, Decker L, Lachapelle F, et al. Progenitor cells of the adult mouse subventricular zone proliferate, migrate and differentiate into oligodendrocytes after demyelination. Eur J Neurosci. 1999; 11:4357–4366. [PubMed: 10594662]
22. Capilla-Gonzalez V, Cebrian-Silla A, Guerrero-Cazares H, et al. The generation of oligodendroglial cells is preserved in the rostral migratory stream during aging. Front Cell Neurosci. 2013 in press.
23. Kojima T, Hirota Y, Ema M, et al. Subventricular zone-derived neural progenitor cells migrate along a blood vessel scaffold toward the post-stroke striatum. Stem Cells. 2010; 28:545–554. [PubMed: 20073084]
24. Arvidsson A, Collin T, Kirik D, et al. Neuronal replacement from endogenous precursors in the adult brain after stroke. Nat Med. 2002; 8:963–970. [PubMed: 12161747]
25. Liu BF, Gao EJ, Zeng XZ, et al. Proliferation of neural precursors in the subventricular zone after chemical lesions of the nigrostriatal pathway in rat brain. Brain Res. 2006; 1106:30–39. [PubMed: 16843444]
26. Nait-Oumesmar B, Picard-Riera N, Kerninon C, et al. Activation of the subventricular zone in multiple sclerosis: evidence for early glial progenitors. Proc Natl Acad Sci USA. 2007; 104:4694–4699. [PubMed: 17360586]
27. Otero L, Zurita M, Bonilla C, et al. Endogenous neurogenesis after intracerebral hemorrhage. Histol Histopathol. 2012; 27:303–315. [PubMed: 22237708]
28. Del Carmen Gomez-Roldan M, Perez-Martin M, Capilla-Gonzalez V, et al. Neuroblast proliferation on the surface of the adult rat striatal wall after focal ependymal loss by intracerebroventricular injection of neuraminidase. J Comp Neurol. 2008; 507:1571–1587. [PubMed: 18236450]
29. Yamashita T, Ninomiya M, Hernandez Acosta P, et al. Subventricular zone-derived neuroblasts migrate and differentiate into mature neurons in the post-stroke adult striatum. J Neurosci. 2006; 26:6627–6636. [PubMed: 16775151]

30. Marti-Fabregas J, Romaguera-Ros M, Gomez-Pinedo U, et al. Proliferation in the human ipsilateral subventricular zone after ischemic stroke. Neurology. 2010; 74:357–365. [PubMed: 20054008]
31. Picard-Riera N, Decker L, Delarasse C, et al. Experimental autoimmune encephalomyelitis mobilizes neural progenitors from the subventricular zone to undergo oligodendrogenesis in adult mice. Proc Natl Acad Sci USA. 2002; 99:13211–13216. [PubMed: 12235363]
32. Gonzalez-Perez O, Romero-Rodriguez R, Soriano-Navarro M, et al. Epidermal growth factor induces the progeny of subventricular zone type B cells to migrate and differentiate into oligodendrocytes. Stem Cells. 2009; 27:2032–2043. [PubMed: 19544429]
33. Kaneko N, Sawamoto K. Neuronal migration in the adult brain. Nihon Shinkei Seishin Yakurigaku Zasshi. 2007; 27:215–218. [PubMed: 18154043]
34. Panagiotakos G, Alshamy G, Chan B, et al. Long-term impact of radiation on the stem cell and oligodendrocyte precursors in the brain. Plos One. 2007; 2:e588. [PubMed: 17622341]
35. Fukuda A, Fukuda H, Swanpalmer J, et al. Age-dependent sensitivity of the developing brain to irradiation is correlated with the number and vulnerability of progenitor cells. J Neurochem. 2005; 92:569–584. [PubMed: 15659227]
36. Tada E, Yang C, Gobbel GT, et al. Long-term impairment of subependymal repopulation following damage by ionizing irradiation. Exp Neurol. 1999; 160:66–77. [PubMed: 10630191]
37. Ford EC, Achanta P, Purger D, et al. Localized CT-guided irradiation inhibits neurogenesis in specific regions of the adult mouse brain. Radiat Res. 2011; 175:774–783. [PubMed: 21449714]
38. Achanta P, Capilla-Gonzalez V, Purger D, et al. Subventricular zone localized irradiation affects the generation of proliferating neural precursor cells and the migration of neuroblasts. Stem Cells. 2012; 30:2548–2560. [PubMed: 22948813]
39. Redmond KJ, Achanta P, Grossman SA, et al. A radiotherapy technique to limit dose to neural progenitor cell niches without compromising tumor coverage. J Neuro-oncol. 2011; 104:579–587.
40. Wong J, Armour E, Kazanzides P, et al. High-resolution, small animal radiation research platform with x-ray tomographic guidance capabilities. Int J Radiat Oncol Biol Phys. 2008; 71:1591–1599. [PubMed: 18640502]
41. Pineda JR, Daynac M, Chicheportiche A, et al. Vascular-derived TGF-beta increases in the stem cell niche and perturbs neurogenesis during aging and following irradiation in the adult mouse brain. EMBO Mol Med. 2013; 5:548–562. [PubMed: 23526803]
42. Brown WR, Thore CR, Moody DM, et al. Vascular damage after fractionated whole-brain irradiation in rats. Radiat Res. 2005; 164:662–668. [PubMed: 16238444]
43. Li YQ, Chen P, Haimovitz-Friedman A, et al. Endothelial apoptosis initiates acute blood-brain barrier disruption after ionizing radiation. Cancer Res. 2003; 63:5950–5956. [PubMed: 14522921]
44. Gonzalez-Perez O, Quinones-Hinojosa A. Dose-dependent effect of EGF on migration and differentiation of adult subventricular zone astrocytes. Glia. 2010; 58:975–983. [PubMed: 20187143]
45. Fike JR, Rola R, Limoli CL. Radiation response of neural precursor cells. Neurosurg Clin N Am. 2007; 18:115–127. [PubMed: 17244559]
46. McGinn MJ, Sun D, Colello RJ. Utilizing X-irradiation to selectively eliminate neural stem/progenitor cells from neurogenic regions of the mammalian brain. J Neurosci Methods. 2008; 170:9–15. [PubMed: 18280577]
47. Gonzalez-Perez O, Alvarez-Buylla A. Oligodendrogenesis in the subventricular zone and the role of epidermal growth factor. Brain Res Rev. 2011; 67:147–156. [PubMed: 21236296]
48. Sanai N, Nguyen T, Ihrie RA, et al. Corridors of migrating neurons in the human brain and their decline during infancy. Nature. 2011; 478:382–386. [PubMed: 21964341]
49. Guerrero-Cazares H, Gonzalez-Perez O, Soriano-Navarro M, et al. Cytoarchitecture of the lateral ganglionic eminence and rostral extension of the lateral ventricle in the human fetal brain. J Comp Neurol. 2011; 519:1165–1180. [PubMed: 21344407]
50. Sanai N, Berger MS, Garcia-Verdugo JM, et al. Comment on “Human neuroblasts migrate to the olfactory bulb via a lateral ventricular extension”. Science. 2007; 318:393. author reply 393. [PubMed: 17947566]
51. Curtis MA, Kam M, Nannmark U, et al. Human neuroblasts migrate to the olfactory bulb via a lateral ventricular extension. Science. 2007; 315:1243–1249. [PubMed: 17303719]

52. Macas J, Nern C, Plate KH, et al. Increased generation of neuronal progenitors after ischemic injury in the aged adult human forebrain. J Neurosci. 2006; 26:13114–13119. [PubMed: 17167100]
53. Gonzalez-Perez O, Gutierrez-Fernandez F, Lopez-Virgen V, et al. Immunological regulation of neurogenic niches in the adult brain. Neuroscience. 2012; 226:270–281. [PubMed: 22986164]
54. Logan TT, Villapol S, Symes AJ. TGF-beta superfamily gene expression and induction of the Runx1 transcription factor in adult neurogenic regions after brain injury. Plos One. 2013; 8:e59250. [PubMed: 23555640]
55. Yan YP, Sailor KA, Vemuganti R, et al. Insulin-like growth factor-1 is an endogenous mediator of focal ischemia-induced neural progenitor proliferation. Eur J Neurosci. 2006; 24:45–54. [PubMed: 16882007]
56. Kang SS, Keasey MP, Arnold SA, et al. Endogenous CNTF mediates stroke-induced adult CNS neurogenesis in mice. Neurobiol Dis. 2012; 49C:68–78. [PubMed: 22960105]
57. Pluchino S, Muzio L, Imitola J, et al. Persistent inflammation alters the function of the endogenous brain stem cell compartment. Brain. 2008; 131:2564–2578. [PubMed: 18757884]
58. Jablonska B, Aguirre A, Raymond M, et al. Chordin-induced lineage plasticity of adult SVZ neuroblasts after demyelination. Nat Neurosci. 2010; 13:541–550. [PubMed: 20418875]
59. Hua G, Thin TH, Feldman R, et al. Crypt base columnar stem cells in small intestines of mice are radioresistant. Gastroenterology. 2012; 143:1266–1276. [PubMed: 22841781]
60. Mohrin M, Bourke E, Alexander D, et al. Hematopoietic stem cell quiescence promotes error-prone DNA repair and mutagenesis. Cell Stem Cell. 2010; 7:174–185. [PubMed: 20619762]
61. Sotiropoulou PA, Candi A, Mascre G, et al. Bcl-2 and accelerated DNA repair mediates resistance of hair follicle bulge stem cells to DNA-damage-induced cell death. Nat Cell Biol. 2010; 12:572–582. [PubMed: 20473297]
62. Schneider L, Fumagalli M, d'Adda di Fagagna F. Terminally differentiated astrocytes lack DNA damage response signaling and are radioresistant but retain DNA repair proficiency. Cell Death Differ. 2012; 19:582–591. [PubMed: 21979466]
63. Ponti G, Obernier K, Guinto C, et al. Cell cycle and lineage progression of neural progenitors in the ventricular-subventricular zones of adult mice. Proc Natl Acad Sci USA. 2013; 110:E1045–E1054. [PubMed: 23431204]
64. Leonard JR, D'Sa C, Klocke BJ, et al. Neural precursor cell apoptosis and glial tumorigenesis following transplacental ethylnitrosourea exposure. Oncogene. 2001; 20:8281–8286. [PubMed: 11781843]
65. Capilla-Gonzalez V, Gil-Perotin S, Garcia-Verdugo JM. Postnatal exposure to *N*-ethyl-*N*-nitrosurea disrupts the subventricular zone in adult rodents. Eur J Neurosci. 2010; 32:1789–1799. [PubMed: 21044178]
66. Capilla-Gonzalez V, Gil-Perotin S, Ferragud A, et al. Exposure to *N*-ethyl-*N*-nitrosourea in adult mice alters structural and functional integrity of neurogenic sites. Plos One. 2012; 7:e29891. [PubMed: 22238669]

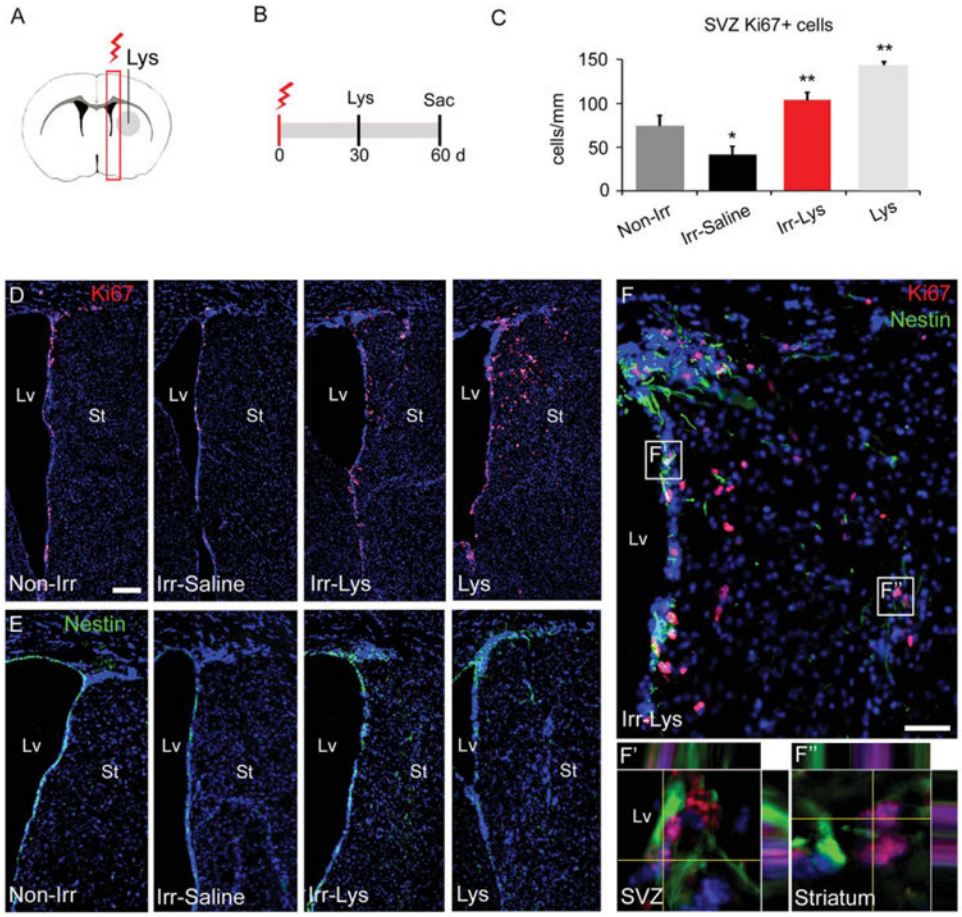

Figure 1.

The locally irradiated SVZ is able to respond to a demyelinated injury. **(A):** Representative coronal section of the mouse brain showing the locally irradiated area (red box) and the demyelinated area (gray area) in the right hemisphere. **(B):** Timeline showing the irradiation protocol, followed by Lys injection. **(C):** Cell quantification of the number of Ki67+ cells in the SVZ. While the Irr-Saline SVZ present a reduced number of Ki67+ cells compared to non-irradiated SVZ, the number of Ki67+ cells increases in mice injected with Lys, even after radiation. **(D):** Representative images of the Ki67 immunoreactivity analyzed in (C). Note the presence of Ki67+ cells in the striatum of the Irr-Lys and Lys hemisphere. **(E):** Immunostaining against the marker Nestin, showing its expression in the SVZ of all groups. Moreover, Nestin+ cells were observed in the striatum of the Irr-Lys and Lys hemispheres. **(F):** Double immunostaining against Ki67 (red) and Nestin (green) in the Irr-Lys hemisphere, showing the presence of double positive cells in the SVZ (representative area in F′) and adjacent striatum (representative area in F″). Scale bar (D, E) = 200 μm, (F) = 50 μm. $*p < .05$; $**p < .01$. Abbreviations: d, day; Lv, lateral ventricle; Lys, Lysolecithin; SVZ, subventricular zone; St, striatum; sac, sacrifice.

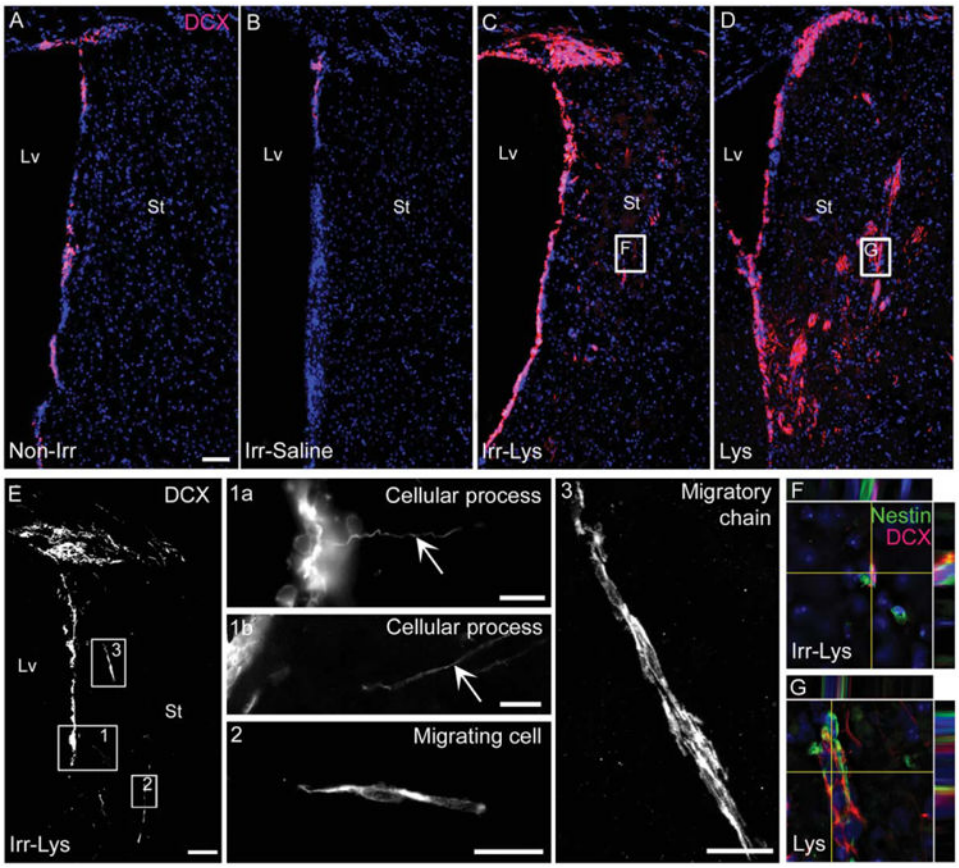

Figure 2.

Abundant neuroblasts were observed in the locally irradiated subventricular zone (SVZ) and in the area of demyelination. Immunofluorescence images of DCX staining. **(A):** SVZ in the non-irradiated hemisphere showing DCX+ cells. **(B):** Irr-Saline SVZ presented a depletion of DCX+ cells. **(C):** The SVZ of Irr-Lys mice showed an increased expression of DCX, presenting DCX+ cells in the striatum. **(D):** The hemisphere injected with Lys shows a high expression of DCX within the SVZ and striatum. **(E):** Localization of the region with DCX+ cells studied in detail in the Irr-Lys mice. (1) DCX+ cells within the SVZ projecting cellular processes toward the adjacent striatum. (2) Elongated DCX+ cell in the striatum of the Irr-Lys hemisphere suggesting that neuroblast migrate from the SVZ. (3) Neuroblasts with elongated morphology formed migratory chain-like structures in the striatum of the Irr-Lys hemisphere. **(F, G):** Double immunostaining against DCX (red) and nestin (green), revealing cells coexpressing both markers in the irradiated (representative area in (F)) and non-irradiated (representative area in (G)) striatum of mice treated with Lys). Scale bar (A–E) = 100 μm, (detail 1a) = 10 μm, (detail 1b) = 20 μm, (detail 2, 3) = 20 μm. Abbreviations: DCX, doublecortin; Lv, lateral ventricle; St, striatum.

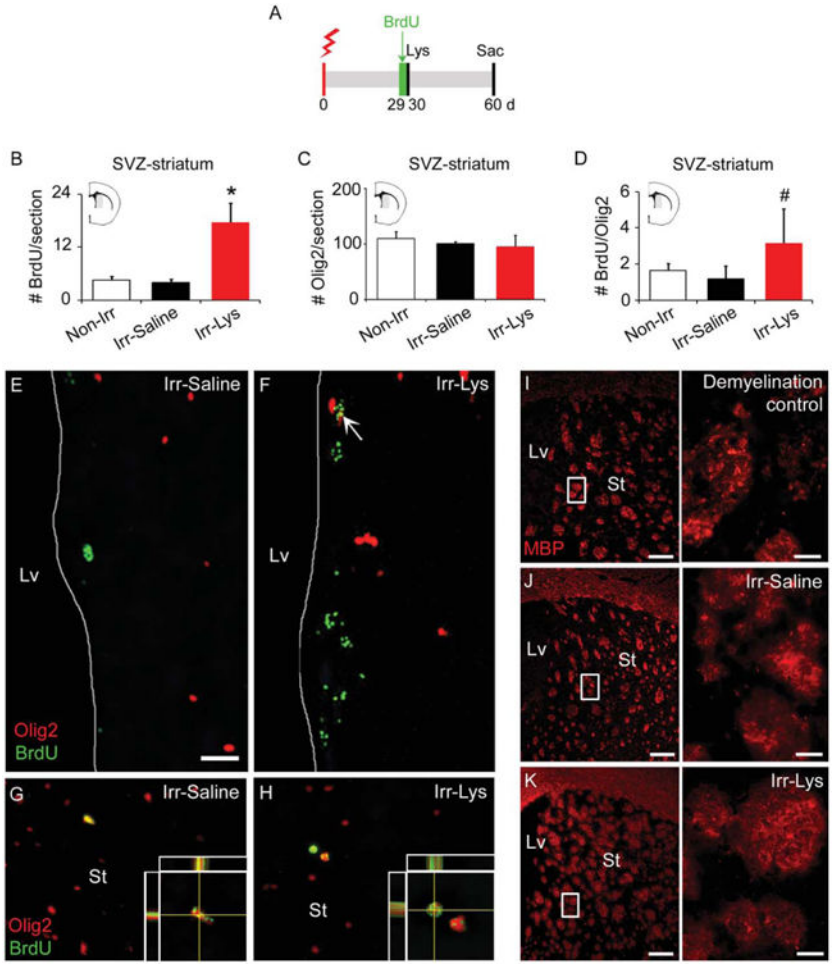

Figure 3.

New Olig2+ cells are found in the irradiated SVZ and within the demyelinated area. **(A):** Timeline for the Lys-treatment combined with radiation and BrdU administration. **(B):** Bar graph representing the number of BrdU+ cells within the SVZ and the adjacent striatum (gray area in brain semisection), 30 days after BrdU administration. Data showed an increase in the Irr-Lys hemisphere, compared to Non-Irr and Irr-Saline hemispheres. **(C):** Bar graph representing the number of Olig2+ cells in the SVZ and adjacent striatum (gray area in brain semisection), 30 days after BrdU administration, showing no differences between groups. **(D):** Bar graph representing the number of BrdU/Olig2+ cells in the SVZ and adjacent striatum (gray area in brain semisection), 30 days after BrdU administration, showing a significant increase in the Irr-Lys hemisphere compared to the non-irradiated hemisphere and an increasing trend compared to the Irr-Saline hemisphere. **(E–H):** Immunostaining against BrdU (green) and Olig2 (red) markers. (E): BrdU/Olig2+ cells were rarely found in the Irr-saline hemisphere. (F): The SVZ of the Irr-Lys hemisphere shows higher number of BrdU+ cells and more frequent BrdU/Olig2+ cells (arrow). (G): Striatum in the Irr-saline hemisphere showing a BrdU/Olig2+ cell. (H): Striatum in the Irr-Lys hemisphere showing BrdU/Olig2+ cells. **(I–K):** Immunostaining against MBP marker. (I): A control demyelinated striatum, 15 days after Lys injection, showing a discontinuous and

fragmented MBP staining. (J): The striatum of the Irr-Saline hemisphere showed a continuous MBP expression. (K): The striatum of the Irr-Lys hemisphere revealed continuous MBP expression 30 days after Lys injection, similar to the Irr-Saline hemisphere. Scale bar (E, F) = 25 μm, (G, H) = 100 μm, (I–K) = 200 μm, details in (I–K) = 20 μm. *Irr-Lys versus all treatments, $p < .05$; #Irr-Lys versus Non-Irr, $p < .05$. Abbreviations: BrdU, 5-bromo-2-deoxyuridine d, day; Lv, lateral ventricle; MBP, myelin basic protein; Olig2, oligodendrocyte transcription factor 2; sac, sacrifice; St, striatum, SVZ, subventricular zone.

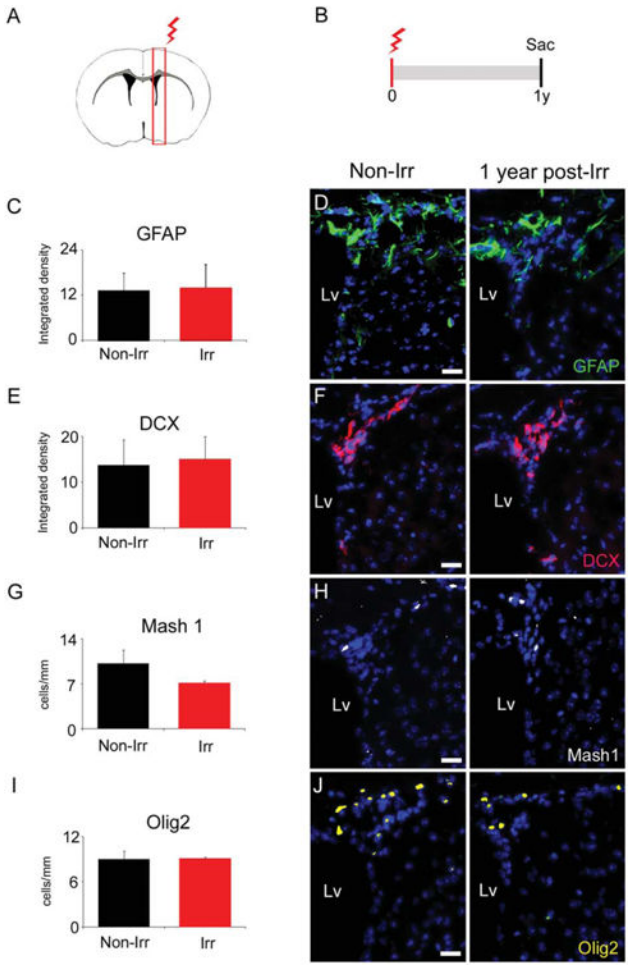

Figure 4.

The remaining cells in the irradiated subventricular zone (SVZ) appear to repopulate the neurogenic niche a year after localized radiation. **(A):** Representative coronal section of the mouse brain showing the locally irradiated area (red box) in the right hemisphere. **(B):** Timeline of radiation delivery and sacrifice of animals. Mice were irradiated with a single dose of 10 Gy and sacrificed a year post-radiation. **(C):** Quantification of GFAP expression showing no differences between irradiated and non-irradiated SVZ a year post-radiation. **(D):** Representative immunohistochemistry images from the quantification in (A). **(E):** Quantification of DCX expression, showing no differences between irradiated and non-irradiated SVZ a year post-radiation. **(F):** Representative immunohistochemistry images from the quantification in (C). **(G):** Quantification of Mash1 expression, showing no differences between irradiated and non-irradiated SVZ a year post-radiation. **(H):** Representative immunohistochemistry images from the quantification in (E). **(I):** Quantification of Olig2 expression, showing no differences between irradiated and non-irradiated SVZ a year post-radiation. **(J):** Representative immunohistochemistry images from the quantification in (G). Scale bar (D), (F), (H), (J) = 20 μm. All comparisons with $p > .05$. Abbreviations: DCX, doublecortin; GFAP, glial fibrillary acidic protein; Lv, lateral ventricle; Olig2, oligodendrocyte transcription factor 2; sac, sacrifice; y, year.

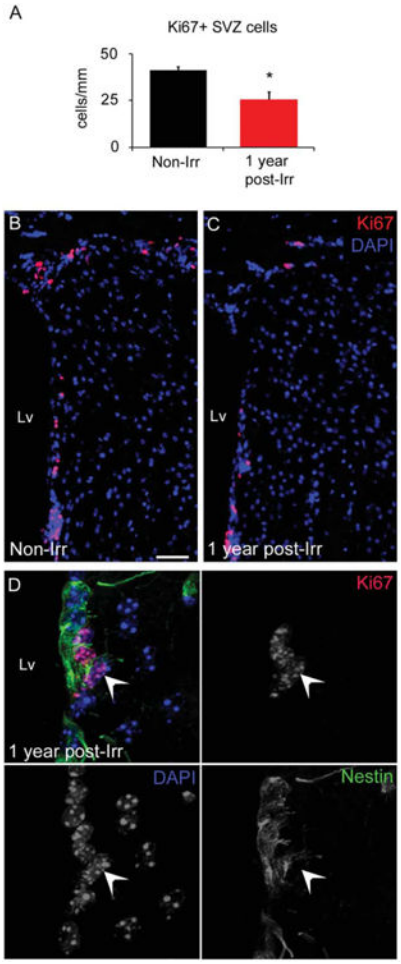

Figure 5.

Proliferative cells are found in the SVZ a year after localized radiation. **(A):** Bar graph depicting the cell quantification of Ki67+ cells in the SVZ, a year post-radiation. **(B, C):** Immunofluorescence images of the Ki67 staining in the non-irradiated and irradiated SVZ. Note the reduced number of Ki67+ cells in the irradiated SVZ. **(D):** Immunostaining against Ki67 (red) and Nestin (green) markers in the irradiated SVZ, a year post-radiation, revealing the presence of double positive cells (arrow). Scale bar (B, C) = 50 μm. *$p < .05$. Abbreviations: DAPI, 4′,6-diamidino-2-phenylindole; Lv, lateral ventricle; SVZ, subventricular zone.

Table 1

Primary antibodies used in this study

Antibody	Species, type	Dilution	Cat. number, manufacturer	Specificity
BrdU	Rat monoclonal, IgG	1:25	Sc-56258, Santa Cruz Biotechnology (Santa Cruz, CA, http://www.scbt.com)	Cells in S-phase
DCX	Rabbit monoclonal, IgG	1:200	4604, Cell signaling Technology (Beverly, MA, http://www.cellsignal.com)	Young neurons
GFAP	Mouse monoclonal, IgG	1:500	MAB360, Millipore (Billerica, MA, http://www.millipore.com)	Astrocyte
Ki67	Rabbit monoclonal, IgG	1:200	RM-9106, Thermo Scientific (Fremont, CA, http://www.thermoscientific.com)	Cells in late G1-, S-, M-, and G2-phases
Mash1	Mouse	1:50	556604, BD Pharmingen (San Jose, CA, http://www.bdbiosciences.com]us.shtml)	Precursor cells
MBP	Chicken polyclonal, IgY	1:200	MBP, Aves Labs Inc (Tigard, OR, http://www.aveslab.com)	Mature oligodendrocytes
Nestin	Mouse monoclonal, IgG	1:100	556309, BD Pharmingen (San Jose, CA, http://www.bdbiosciences.com)	Stem cells
Olig2	Rabbit polyclonal, IgG	1:500	AB9610, Millipore (Billerica, MA, http://www.millipore.com)	Young oligodendrocytes
Sox2	Mouse monoclonal, IgG	1:50	MAB2018, R&D System (Minneapolis, MN, http://www.rndsystems.com)	Stem cells

Abbreviations: BrdU, 5-bromo-2-deoxyuridine; DCX, doublecortin; GFAP, glial fibrillary acidic protein; MBP, myelin basic protein